

Determination of the Elastic-Plastic Fracture Mechanics Z-factor for Alloy 182 Weld Metal Flaws for Use in the ASME Section XI Appendix C Flaw Evaluation Procedures

G. Wilkowski, H. Xu, D.-J. Shim, and D. Rudland

Engineering Mechanics Corporation of Columbus
3518 Riverside Dr. - Suite 202
Columbus, Ohio

ABSTRACT

One of the ways that the ASME Section XI code incorporates elastic-plastic fracture mechanics (EPFM) in the Section XI Appendix C flaw evaluation procedures for circumferential cracks is through a parameter called Z-factor. This parameter allows the simpler limit-load (or net-section-collapse) solutions to be used with a multiplier from EPFM analyses. Traditionally the EPFM solution was determined by using the GE-EPRI J-estimation scheme to determine the maximum load by EPFM, and $Z = \text{limit load} / \text{EPFM solution}$. The Z-factor is a function of the material toughness as well as the pipe diameter.

With the advent of primary water stress-corrosion cracks (PWSCC) in pressurized water reactor (PWR) dissimilar metal welds (DMW), there is a need to develop Z-factors for Alloy 82/182 nickel-based alloy welds that are susceptible to such cracks. Although there have been Z-factor solutions for cracks in stainless and ferritic pipe butt welds, the DMW are somewhat different in that there is a much lower yield strength material on one side of the weld (typically forged or wrought 304 stainless steel) and on the other side of the weld the low alloy steel has a much higher strength than even the weld metal.

This paper shows how 3D finite element analyses were used for a particular pipe size to determine the sensitivity of the crack location in the Alloy 182 weldment (crack in the center of weld, or closer to the stainless or low alloy steel sides), and how an appropriate stress-strain curve was determined for use in the J-estimation schemes. A Z-factor as a function of the pipe diameter was then calculated using the LBB.ENG2 J estimation scheme using the appropriate stress-strain curves from the finite element analysis. The LBB.ENG2 analysis was used rather than the GE-EPRI estimation scheme since it has been found that the LBB.ENG2 analysis is more accurate when compared with full-scale pipe tests. From past work, the GE-EPRI method was found to be the most conservative of the J-estimation schemes in predicting the maximum loads for circumferential flaws when compared to full-scale circumferentially cracked-pipe tests. The proposed Z-factor relationship should be restricted to normal operating

temperatures (above 200C) with low H_2 concentrations, where the Alloy 182 weld metal exhibits high toughness.

BACKGROUND

The occurrence of PWSCC in dissimilar metal pipe butt welds using Alloy 82 and 182 weld metals has been increasing and evaluation procedures are needed in Section XI of the ASME Boiler and Pressure Vessel Code. Article IWB-3640 and Appendix C (2004 Edition) cover elastic-plastic fracture mechanics (EPFM) analyses for ferritic and austenitic stainless steels and their welds. Currently no criterion exists for cracks in Alloy 82/182 weld metals.

The existing ASME elastic-plastic fracture mechanics analyses include a relatively simple procedure where there is a correction factor for the EPFM failure stress relative to that calculated by limit-load. The correction factor is called a Z-factor, which is a function of the material toughness as well as the pipe diameter. The Z-factor is the ratio of the nominal stress calculated by net-section-collapse method divided by the nominal stress calculated by EPFM.

The early work on the development of a Z-factor used the GE/EPRI circumferential through-wall-cracked pipe solutions where the pipe was loaded in bending [1]. In that work it was recognized that the maximum load ratio of limit-load to the GE/EPRI [2] EPFM predictions varied with crack length, but had a maximum ratio for a crack that was 25 to 30% of the circumference. For simplicity and conservatism, this maximum ratio of the limit-load/EPFM maximum loads was taken as the Z-factor. This Z-factor also increased with pipe diameter, and would be higher for lower toughness materials.

It should also be noted that for cracks in welds, some earlier FE analyses and experimental results showed that the applied crack-driving force (J-applied) was best calculated by using the base-metal stress-strain curve rather than the weld metal stress-strain curve together with the weld metal J-R curve to predict the fracture behavior [3].

Some other relevant results since the early development of the ASME Z-factors are discussed below.

- Statistically it was shown that stainless steel shielded metal arc welds (SMAW) had the same toughness as submerged arc welds (SAW), so Z-factors for those two welds were made identical in a more recent version of Section XI Appendix C.
- A large number of full-scale pipe tests were conducted and compared to a variety of J-estimation analyses [4]. These results showed that the GE/EPRI J-estimation scheme was the most conservative in predicting maximum loads for circumferentially cracked pipes. The method that was the most accurate was the one developed at Battelle called the LBB.ENG2 method [5].
- Experimental and analytical work in [6] showed that the Code developed ferritic pipe Z-factors [7] are very conservative. Although this is not the topic of this paper, these ferritic pipe Z-factors should be updated.
- There was only one dissimilar metal weld full-scale pipe fracture test conducted with Alloy 182 weld metal. This was a 36-inch diameter by 3.36 inch thickness A516 Grade 70 cold leg pipe from a canceled CE plant with a forged stainless steel safe end with an Alloy 182 weld [8], as shown in Figure 1. A circumferential through-wall crack was inserted along the fusion line of the ferritic material and the Inconel buttering. (At that time there was a concern about HAZ toughness in DM welds.) Those results showed that the load at crack initiation, maximum loads, and entire load-displacement behavior during the large crack growth could be best predicted by using the A516 Grade 70 base metal stress-strain curve rather than the weld metal stress-strain curve, see Figure 2.

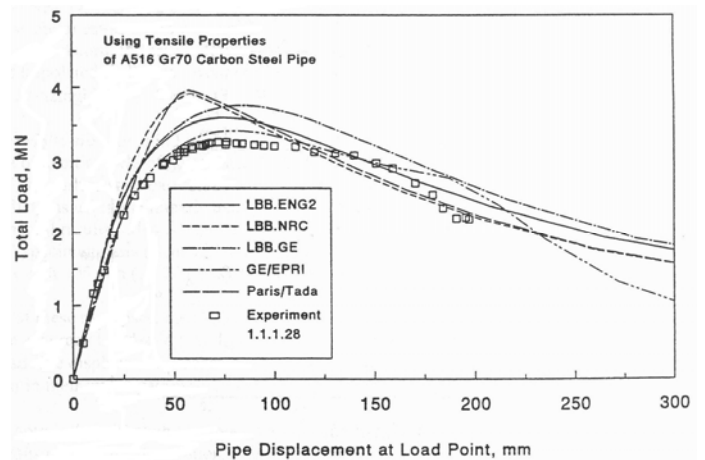


Figure 2 Comparison of predicted and experimental load-displacement curves from circumferential through-wall cracked pipe test under 4-point bending at 550F. (Reproduced from [8])

RECENT ALLOY 82/182 FRACTURE TOUGHNESS DATA

In recent years, there has been more interest in the possibility of cracks in the Alloy 82/182 weld metal itself, rather than the fusion line or HAZ. J-R curve data were developed by Battelle in [9] at quasi-static loading conditions in air environment. This was done on the same weld as shown in Figure 1. The specimens were 1T CT specimens with the crack in either the center of the weld, or in the center of the buttered region. Additionally, the orientations corresponded to radial crack growth or circumferential crack growth. The J-R curve results at 315C (600F) showed essentially no difference with cracks at different locations or orientations in the weld, and were actually higher in toughness than the fusion-line crack location, see Figure 3.

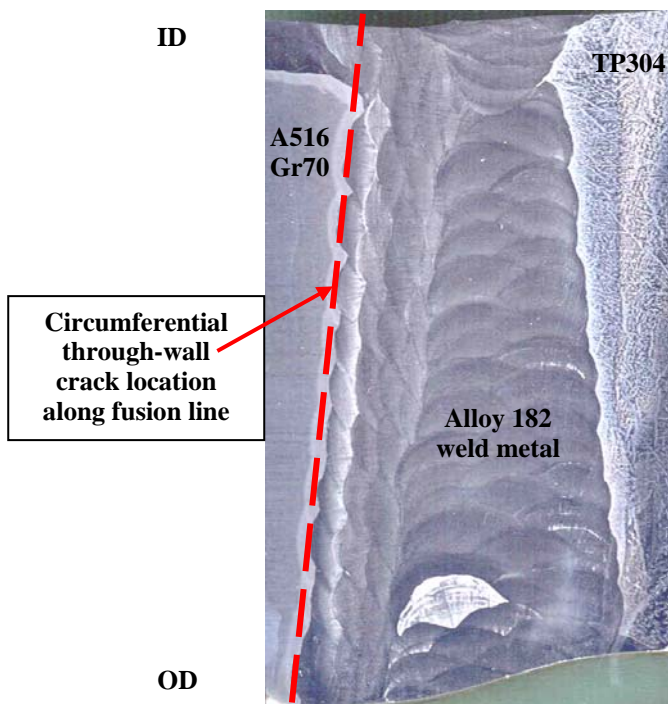


Figure 1 Dissimilar weld in cold-leg pipe fracture test

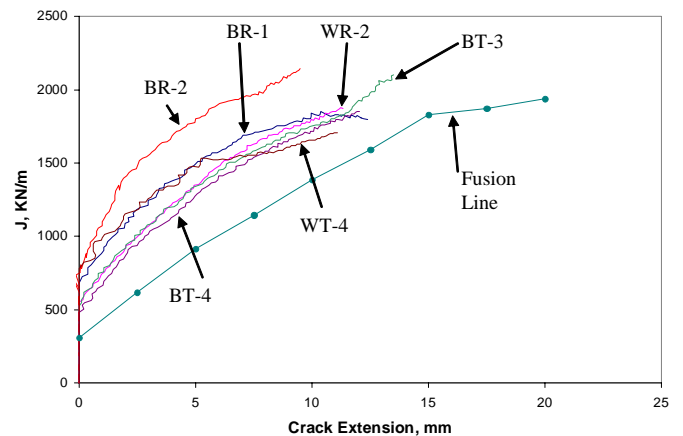


Figure 3 J-R curves for Alloy 182 weld shown in Figure 1 (Reproduced from [9])

(B = crack in butter, W = crack in centerline of weld, R=radial crack growth direction, T = circumferential through-wall growth direction)

Another recent source of Alloy 82 weld metal toughness data is the work done at Bettis Labs by Mills and Brown [10]. In this work, the authors examine the toughness of Alloy 82 welds at higher and lower temperatures than the Battelle work, but also did testing in air and water, where the water had up to 150 cc of H₂ per kg of H₂O and the test specimens were precharged to reach the desired hydrogen concentrations. Tests were also done at slow and fast strain rates.

The results of the testing showed that at 336C (637F) in air environment, the toughness was high and comparable to the Alloy 182 J-R curves in [9]. At slow rates and at lower temperatures with the higher hydrogen concentrations, the calculated J-R curves could be lower in toughness by several orders of magnitude, see Figure 4. For these same temperature and hydrogen levels at high rate testing the toughness returned to the higher value.

These results suggest that any EFPM analyses developed for Code applications should be limited to lower hydrogen environmental conditions. The higher hydrogen environmental conditions (if even possible in a power plant), could correspond to linear elastic fracture mechanics conditions, where weld residual stresses might be important.

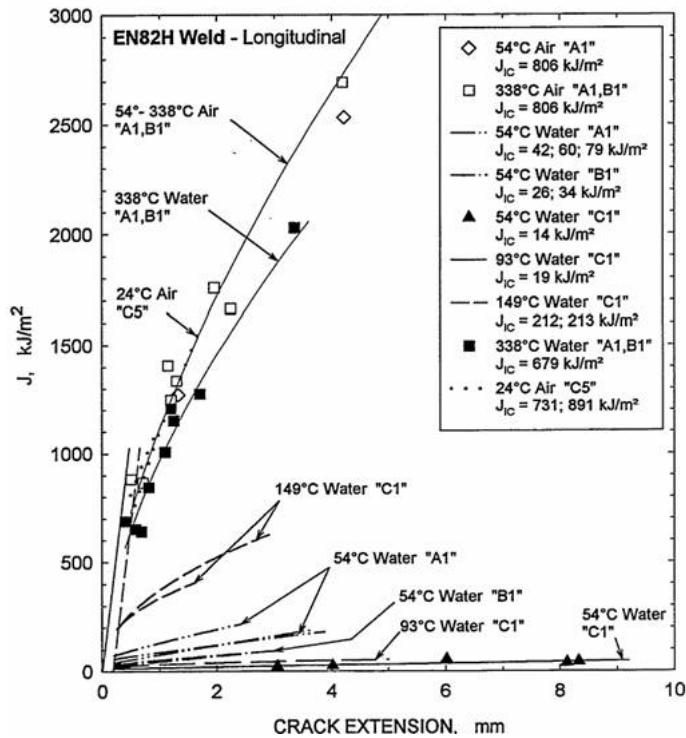


Figure 4 J-R curve testing results on Alloy 82 weld metal from Mills (Reproduced from [10])

INVESTIGATION IN THIS PAPER

The evaluations performed in this effort involved conducting FE analyses for circumferential through-wall cracks in dissimilar metal welds of a surgeline pipe. These calculations

demonstrated which stress-strain curve should be used in the J-estimation schemes in order to predict the J-moment response. In past flawed-pipe weld analyses, the base-metal properties were the same on both sides of the weld. In the dissimilar metal welds, the base metal properties can be drastically different on the two sides of the weld.

Finite Element Analysis Results

The FE analysis was on 14-inch outer diameter by 1.246-inch wall thickness pipe with an internal pressure of 2,250 psig. The total circumferential through-wall crack was kept as 6 inches (3-inch in half symmetry model) for all FE analyses.

To provide guidance on which base metal stress-strain curves should be used in the J-estimation schemes for the Z-factor determination, the crack was located in three different axial locations, i.e., the center of the weld, close to the ferritic side, and close to the stainless-steel safe-end side. A mesh generator developed by the authors was used, along with the ABAQUS FE solver. The different crack locations in the welds are shown in Figures 5 to 7. The case in Figure 7 also was done with A516 Grade 70 ferritic base metal rather than the A508 nozzle material. In the first two crack location cases, the weld bevel was held at 22-degrees (typical of actual welds). To get the crack located close to the ferritic base metal, the mesh generator had to use the configuration shown in Figure 7, which is more of an idealized rectangular cross-section of the weld area.

For all three cases, the pipe length was assumed to be 100-inches. A separate analysis with a pipe length of 160-inches showed almost identical results. This was done to insure that the bending-moment boundary conditions were correct.

Based on past experience [3], for crack stability analyses, the weld residual stresses need not to be included for materials having the toughness levels of the Alloy 82/182 welds at the higher temperatures. Hence this analysis is not valid for the case of lower temperature water with the higher hydrogen concentrations that give the very low toughness results shown in Figure 4.

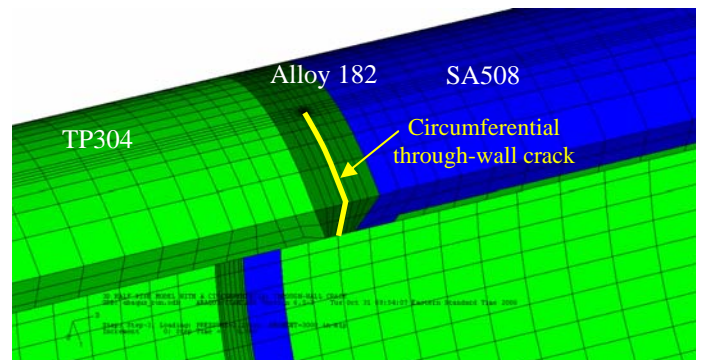


Figure 5 Circumferential through-wall crack in center of Alloy 182 weld in surge line (focused mesh at crack tip)

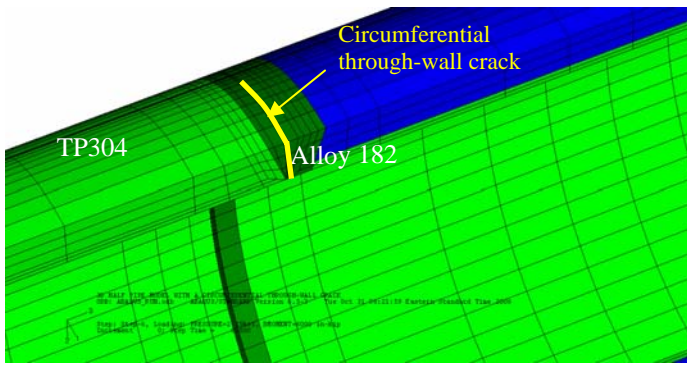


Figure 6 Circumferential through-wall crack closer to TP304 safe end in surge line

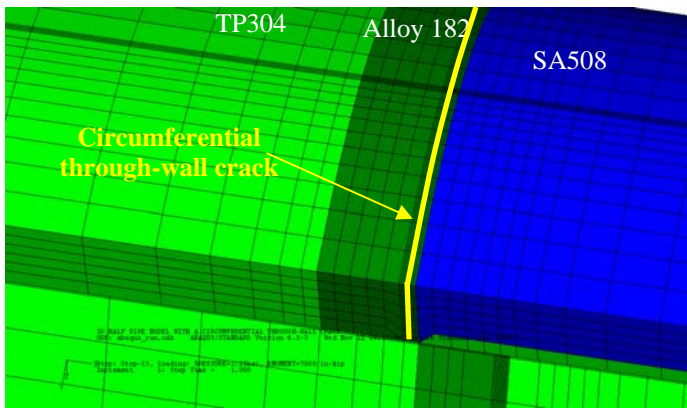
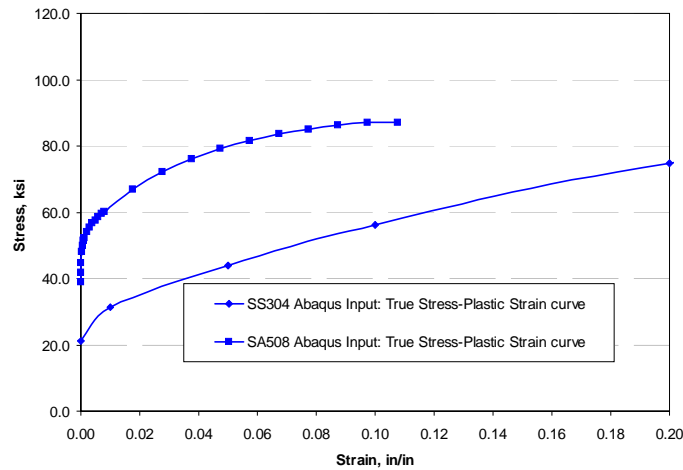
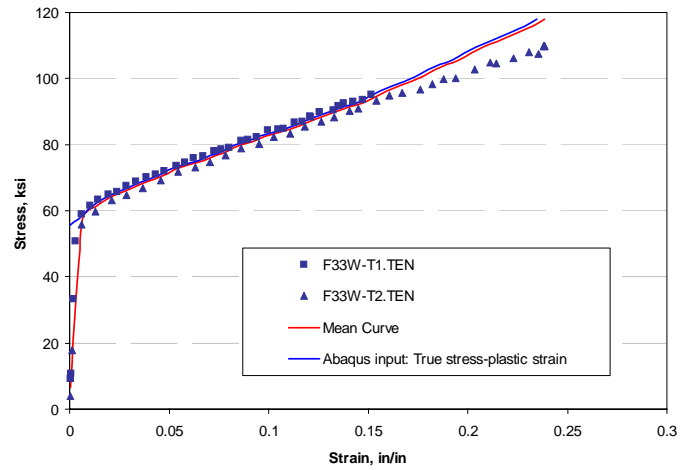


Figure 7 Circumferential through-wall crack closer to A508 nozzle material in surge line

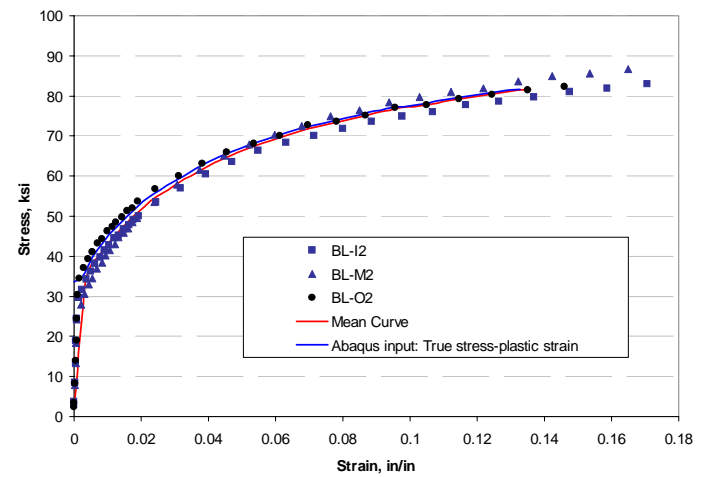
The actual stress-strain curves of A508 nozzle material, as-welded Alloy 182 weld metal, and TP304 safe end material were used. In one case, A516 Grade 70 base metal was used on the ferritic side. The stress-strain curves at 288C to 315C are shown in Figure 8.



(a) TP304 and A508 base metals (315C)



(b) Alloy 182 weld metal in as-welded condition (288C)



(c) A516 Grade 70 ferritic base metal (288C)

Figure 8 Actual stress-strain curves for various materials, (1 ksi = 6.895 MPa, 1 in = 25.4 mm)

Comparison to J-estimation Schemes

As noted in the Background Section, the original Z-factors [1] were calculated by the GE/EPRI method. Shortly afterwards, it was found in the NRC-funded full-scale test programs[4], that the GE/EPRI J-estimation scheme was the most conservative procedure, whereas the LBB.ENG2 analysis by Battelle [5] was the most accurate for circumferential through-wall-cracked pipes. Hence in the following analyses, the LBB.ENG2 method was used.

In the dissimilar metal weld case, there are significantly different base metals on either side of the weld. Therefore, the pipe base-metal stress-strain curve in the J-estimation scheme needs to be selected to give the same J-integral crack-driving force as the detailed FE analyses.

A comparison of the J versus moment curves from the FE analyses with the LBB.ENG2 analysis is shown in Figure 9 for the case of the crack in the center of the weldment (including buttered region). These results showed that for the crack in

this location, the FE J-moment curve is between that from using the TP304 base-metal stress-strain curve, and the weld metal or A508 base-metal stress-strain curves. An equivalent stress-strain curve that was a weighted average of the TP304 and A508 material properties was found to give the same crack-driving force in the LBB.ENG2 analysis as the FE analyses. In the case of the crack in the center of the weld and using A508 ferritic nozzle material, the equivalent material properties (yield strength, ultimate strength, elastic modulus and R-O parameters) are given as $\text{Equivalent} = \text{TP304} * 0.6 + \text{A508} * 0.4$.

Using the equivalent stress-strain curve on the LBB.ENG2 method gave the blue curve in Figure 9 that is virtually identical to the FE results.

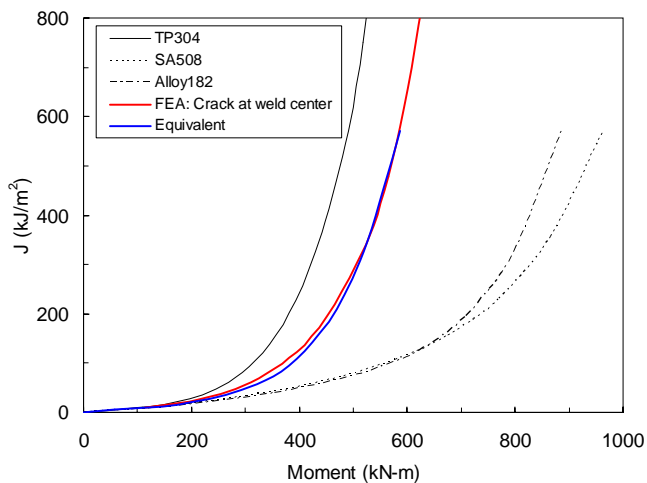


Figure 9 Comparison of FE and LBB.ENG2 J-moment curves for the case of a crack located in the center of the weld with A508 ferritic nozzle material

The results from all of the FE analyses and comparison with LBB.ENG2 J-estimation scheme predictions are given in Figure 10. This shows the results from Figure 9 as well as the cases of having the cracks located closer to the TP304 safe end, or closer to the ferritic steel (A516 Gr70 pipe or A508 nozzle material). The interesting aspect of this exercise was that if the crack was in the weld but closer to the stainless-steel safe end, then the LBB.ENG2 method using the stainless steel stress-strain curve agreed with the FE J-moment curve. Additionally, if the crack was in the weld but closer to the ferritic nozzle (i.e., in the buttering) then the LBB.ENG2 analysis agreed with the FE J-moment curve when the average of the A508 and TP304 stress-strain curves was used.

DETERMINATION OF Z-FACTORS

From the prior comparisons of the FE analyses with the LBB.ENG2 J-estimation scheme, an effective stress-strain curve could be properly applied to calculate the EPFM maximum loads that are used in the Z-factor determination. Since the crack could be anywhere in the weldment, we used the conservative assumption that it could be closer to the TP304 safe-end, which means that *the TP304 stress-strain curve is used in the calculations, and that the TP304 stainless steel flow stress is used in the limit-load calculations.* The flow stress

was taken as the average of yield and ultimate strength, which is consistent with comparisons of flow-stress values directly from pipe tests and comparisons to tensile test data.

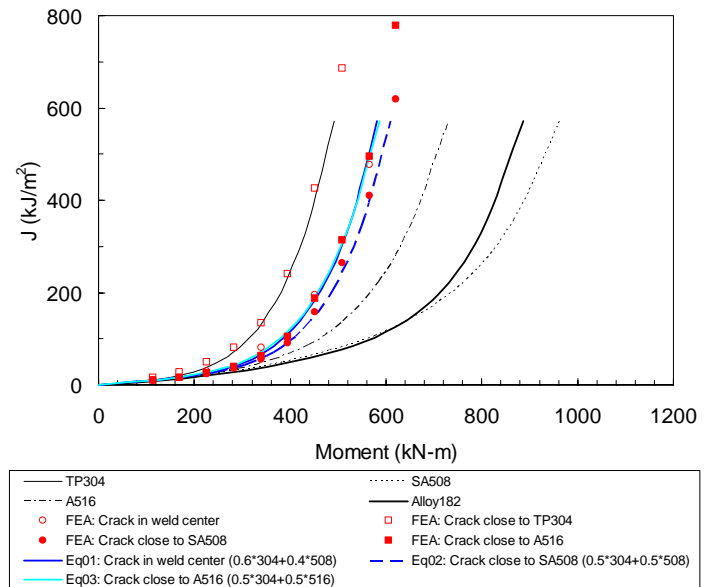


Figure 10 Comparison of all FE analyses and equivalent stress-strain curve matches from the LBB.ENG2 method

The Z-factor determination involves calculating the nominal stress by net-section-collapse analysis and the nominal stress calculated by EPFM. This is done as a function of pipe diameter. At each diameter, several crack lengths were used to determine the maximum limit-load/EPFM ratio. That maximum ratio is the Z-factor for that diameter. The result of this set of calculations is presented in Figure 11, and essentially is the same results derived in [11] other than the curve-fit equation given here. The Z-factor equation for the Alloy 182 weld cracks is given in Equation 1. This equation was developed so that there was a smooth transition at 8-inch diameter, and the average error in the curve fit compared to the calculated data points was 0.1 percent.

A comparison of this Z-factor equation and those in the existing ASME Section XI analyses for stainless steel welds as well as ferritic pipe base metal and welds is given in Figure 12. Note that the shape of the new curve is considerably flatter than the original equations, which is the reason why a two-segment curve-fit equation had to be used. Also the Alloy 182 weld metal Z-factor curve is much lower than any of the other ASME Z-factors curves mainly because of the higher toughness of the Alloy 182 weld metal than the stainless steel welds or ferritic weld/base metals. As noted earlier, the higher Z-factor values in the ASME Z-factor curves with increasing diameter is due to the use of the more conservative GE/EPRI estimation scheme in the derivation of the earlier Z-factors.

$$Z = 0.00065 * D^3 - 0.01386 D^2 + 0.1034 * D + 0.902 \text{ for } D \leq 8'' \quad (1a)$$

$$Z = 0.000022 D^3 - 0.0002 D^2 + 0.0064 D + 1.1355 \text{ for } D \geq 8'' \quad (1b)$$

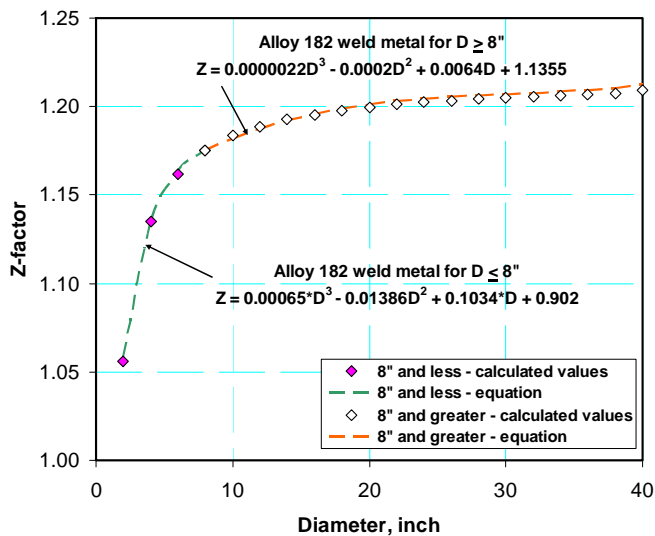


Figure 11 Calculated Alloy 182 Z-factors at different diameters and curve-fit equations

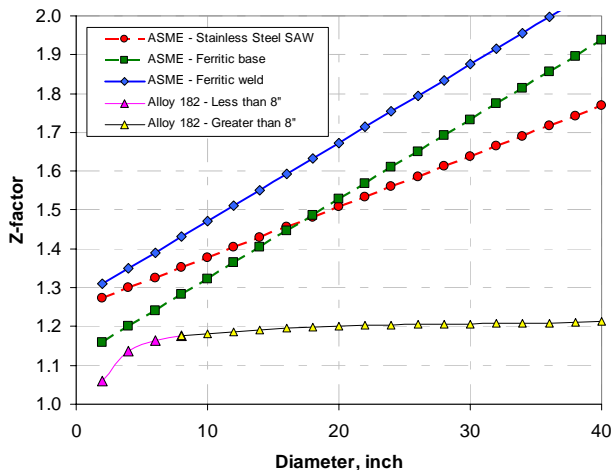


Figure 12 Comparison of proposed Alloy 182 weld crack Z-factor to existing ASME Z-factors for stainless welds and ferritic pipe

CONCLUSION

The work in this paper presents new Z-factor equations for EPFM flaw evaluation of cracks in Alloy 182 that could be used in Section XI of the ASME Code. FE analyses were used in this evaluation to determine the appropriate stress-strain curve to be used for the dissimilar metal weld crack case where there are drastically different base metal strengths on either side of the weld. The FE validation analyses showed that the crack-driving force can change with the location of the crack within the weld, i.e., in the center of the weld, or closer to the stainless-steel safe end or the nozzle ferritic material. The Z-factors developed in this paper assume that the crack is located close to the safe end, which is the most conservative case. The Alloy 182 Z-factor weld curve is also contingent on using the higher J-R curves at normal operating temperatures,

and should not be applied to operating conditions for lower temperatures in combination with higher hydrogen combinations. In the Code evaluation procedures, the stainless steel properties should be used in the limit-load analysis. The much lower Z-factor curve shape relative to the current ASME Z-factor curve for other materials is due to the higher toughness of the Alloy 182 weld metal and using the more accurate J-estimation scheme than the conservative analysis used in the earlier ASME Z-factor development. Finally, this exercise points out that the past conclusions regarding to the Z-factor relationship for ferritic pipe and welds should probably be updated.

ACKNOWLEDGEMENTS

The authors would like to thank the Nuclear Regulatory Commission for their support of this work.

REFERENCE

1. "Evaluation of Flaws in Austenitic Steel Piping," (Technical basis document for ASME IWB-3640 analysis procedure), prepared by Section XI Task Group for Piping Flaw Evaluation, EPRI Report NP-4690-SR, April 1986.
2. Kumar, V., and others, "An Engineering Approach for Elastic-Plastic Fracture Analysis," EPRI Report NP-1931, July 1981.
3. Wilkowski, G. M., and others, "Analysis of Experiments on Stainless Steel Flux Welds," NUREG/CR-4878, April 1987.
4. Wilkowski, G. M., Olson, R. J., and Scott, P. M., "State-of-the-Art Report on Piping Fracture Mechanics," U.S. Nuclear Regulatory Commission report NUREG/CR-6540, BMI-2196, February 1998.
5. Brust, F. W., "Approximate Methods for Fracture Analyses of Through-Wall Cracked Pipes," NRC Topical Report by Battelle Columbus Division, NUREG/CR-4853, February 1987.
6. Choi, Y. H., Lee, J. B., and Wilkowski, G. M., "Development of New Z-factors for the Evaluation of a Surface Crack in Nuclear Piping," SMiRT 14, Volume G, pp 603-610, August 1997.
7. "Evaluation of Flaws in Ferritic Piping," EPRI Report NP-6045, prepared by Novetech Corporation, October 1988.
8. Scott, P. M., and others, "Fracture Evaluations of Fusion Line Cracks in Nuclear Pipe Bimetallic Welds," NUREG/CR-6297, April 1995.
9. C. Williams, F. Brust, P. Scott, D. Rudland, G. Wilkowski, R. Tregoning, and C. Santos, "The Impact of Fracture Toughness and Weld Residual Stresses of Inconel 82/182 Bimetal Welds on Leak-Before-Break Behavior," 2004 ASME PVP Conference.
10. W. J. Mills and C. M. Brown, "Fracture Toughness of Alloy 600 and EN82H Weld in Air and Water," U.S. Department of Energy Contract DE-ACII-98PN38206, June 1999.
11. G. Wilkowski, H. Xu, P. Krishnaswamy, N. Chokshi, S. Shaikat, A. Hiser, G. DeGrassi, J. Johnson, and R. Olson, "Seismic Considerations for the Transition Break Size," presented at 2006 ASME PVP conference.